Iraqi Geological Journal

Journal homepage: https://www.igj-iraq.org

Geology, Pb and S Isotope Geochemistry, and Genesis of the Na Bop-Pu Sap Lead-Zinc Deposit in the Cho Don area, Northeastern Vietnam

Khuong T. Hung[1,*], Le Xuan Truong[1], Salih M Awadh[2], Ta Van Thang[3], Ngo Xuan Dac[4], Nguyen Khac Du[1]

[1] Hanoi University of Mining and Geology, Vietnam
[2] Department of Geology, College of Science, University of Baghdad, Baghdad, Iraq
[3] Intergeo Division, Department of Mineral Resources, Vietnam
[4] Vietnam Institute of Geosciences and Mineral Resources, Vietnam
* **Correspondence**: khuongthehung@humg.edu.vn

Received:
26 March 2023

Accepted:
10 May 2023

Published:
30 September 2023

Abstract

The Na Bop-Pu Sap Pb-Zn ore bodies represent a typical vein-type lead-zinc deposit situated in the Cho Don area and are currently being extracted for their lead and zinc resources. This deposit is characterized by its significant scale and quality and is considered one of the prominent lead-zinc deposits in the Cho Don area. Despite its significance, this deposit has not received adequate attention, resulting in limited knowledge of its geology, mineralization, and deposit genesis model. To address this knowledge gap, our study utilized several methodologies, including field surveying, ore mineral analysis under a microscope, and S and Pb isotopic geochemistry. By employing these approaches, we were able to obtain specific insights into the origin of mineralization and the deposit model. Our field survey suggests that the ore deposits are formed as Pb-Zn-bearing veins along Devonian shale, claystone, and limestone faults. Microscopic analyses of the veins reveal the presence of galena, sphalerite, chalcopyrite, pyrite, arsenopyrite, and pyrrhotite as ore minerals, and quartz, calcite, dolomite, and chalcedony as gangue minerals. Sulfur-isotope values ($\delta^{34}S_{CDT}$) of galena 5.3 to 0.1‰ (average 2.8‰), sphalerite 6.8 to 2.5‰ (average 5.3‰), and pyrite 5.8 to 4.1‰ (average 4.9‰) indicate that the sulfide mineralization may be related to a deep source, possibly originating from magmatic activity in the region and contaminated by carbonate-bearing marine sedimentary rocks. Lead-isotope studies indicate a model age of 598-424 Ma for the lead reservoir, consistent with the possible presence of local source rocks containing sulfur. The lead and sulfur in the ore veins were probably contaminated by Devonian carbonate-bearing marine sedimentary rocks and leached from Neoproterozoic to Cambrian magmatic activity. The lead-zinc deposits in Na Bop-Pu Sap do not display any Mississippi valley-type (MVT) or Sedimentary exhalative (SEDEX) lead-zinc deposit characteristics, as they appear to be related to shear zone-hosted lead-zinc deposits.

Keywords: Sulfur; Lead isotopes; Lead-zinc deposit; Na Bop-Pu Sap deposit

DOI: 10.46717/igj.56.2C.13ms-2023-9-19

1. Introduction

Sedimentary exhalative (SEDEX) and Mississippi valley-type (MVT) mineralization are the most important sources of Pb-Zn deposits globally (Wilkinson, 2013). These types of ore deposits are sedimentary to diagenetic in origin and often contain laminated sulfides parallel to bedding and sedimentary features such as graded beds (Leach, 2005). The formation of these deposits is a complex geological process that involves the migration, deposition, and alteration of metals and minerals within the Earth's crust. Therefore, understanding these deposit's genesis, age, and formation history is crucial for effective mineral exploration, mining, and environmental management (Sangster et al., 2011; Milot et al., 2019; Ünal-Çakır, 2020; Hung, 2021; Duong et al., 2021). Vietnam's Cho Don-Cho Dien mining area is known for its abundant lead-zinc resources, found in numerous deposits and occurrences (Tri et al., 2011; Hung et al., 2020a&b). While most of these deposits are situated in early and middle Devonian carbonate rocks, more research has focused on the Cho Dien rather than the Cho Don area. Therefore, further research is needed to fully understand the geology and mineralization of the Cho Don-Cho Dien mining area, particularly in the under-investigated Cho Don area.

The Cho Don area, located in the southern Bac Kan province, includes several deposits such as Na Bop-Pu Sap, Na Tum, Ba Bo, and Lung Vang. Among these deposits, the Na Bop-Pu Sap one is distinguished by its remarkable size and quality and is regarded as one of the prominent lead-zinc deposits in the Cho Don area. Previous studies have classified ore deposits in the Cho Don-Cho Dien mining areas into MVT deposits (Hoa et al., 2010), sediment-hosted deposits (Hung et al., 2021), or even SEDEX deposits (Binh, 2005; 2010). In the 1980s of the 20th centuries, Vinh (1982) has been found that granitoid rocks in the Cho Don area exhibit high concentrations of Pb and Zn, which are 3 to 4 times higher than the Clark values. The U-Pb isotopic dating of zircon in the Phia Bioc granite complex indicates an age range of 200-280 Ma, while the model age of galena from the Cho Don-Cho Dien area yields an age range of 215-226 Ma (Vinh, 1982). Furthermore, Niem (2010) has reported an increase in the formation temperature of zinc-lead ore from the central fold hinge of Phia Khao to the east, where granite masses of the Phia Bioc complex are distributed. These findings suggest that the Na Bop-Pu Sap lead-zinc deposit may be associated with the granitoid blocks of the early Triassic Phia Bioc complex. More recent studies have classified them as Pb-Zn hydrothermal deposits, based on the mineral assemblage and trace element characteristics (Ishihara et al., 2010; Anh et al., 2012; Can et al., 2014). The above evidence suggests that the genesis of the Na Bop-Pu Sap deposit is a contentious matter that requires further clarification. This study aims to elucidate the geological, mineralogical, and genesis of Pb-Zn ores, along with their sulfur and lead isotopic geochemical characteristics. This will be achieved through a combination of field surveying, ore mineral analysis under a microscope, and S and Pb isotopic geochemistry.

2. Geological Background

The Lo Gam structural zone is situated on the southeastern margin of the Yangtze platform, which includes the early Proterozoic crystalline basement (Golonka et al., 2006). During the early Paleozoic-Devonian, this zone was located at the periphery of the South China epicontinental sea, where it was a submarine carbonate upland with predominant shallow-water terrigenous sedimentation. The collision of continental blocks of the Yangtze and Cathaysia during the Permian-Triassic led to the involvement of early Paleozoic-Devonian sedimentary formations in intraplate fold-and-thrust orogeny, and the Lo Gam block occupies the southwestern flank of the South China intracratonic orogeny structure (Hoa et al., 2008). The early-middle Triassic tectonic-magmatic activation of the Lo Gam structural zone emphasizes its orogenic origin, characterized by the synchronization and spatial juxtaposition of granitoid and mafic-ultramafic intrusive magmatism (Vladimirov et al., 2012). The Cho Don area is

situated in the northeastern region of Vietnam, within the eastern Lo Gam structural zone or Phu Ngu zone (Tri et al., 2011). The region is underlain by early Devonian carbonate rocks (Figs. 1A, B).

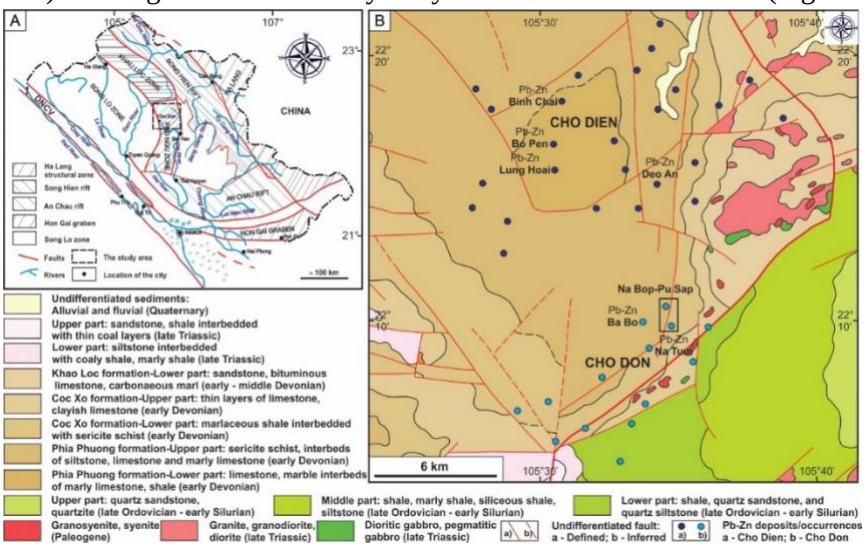

Fig. 1. (A) Tectonic sketch map of northeastern Vietnam, showing the location of the Cho Don-Cho Dien area (adapted from Tri et al. 2011); (B) Locations of the lead-zinc deposits and occurrences in the Cho Don-Cho Dien area (modified from Quoc et al., 2000; Bac, 2011).

The Na Bop-Pu Sap mining area is located in the Cho Don area and consists predominantly of terrigenous sedimentary formations with phyllite-quartzite interbeds and sandstone layers of the late Ordovician-early Silurian Phu Ngu formation. The lead-zinc ore bodies mainly occur in the limestone layers of the Coc Xo formation. Phyllite-quartz-sericite interbedded with sandstone layers, quartzite-cemented sandstone, thin limestone layers, white marble, and light grey limestone of the early Devonian Coc Xo formation are also common in this region (Quoc et al., 2000).

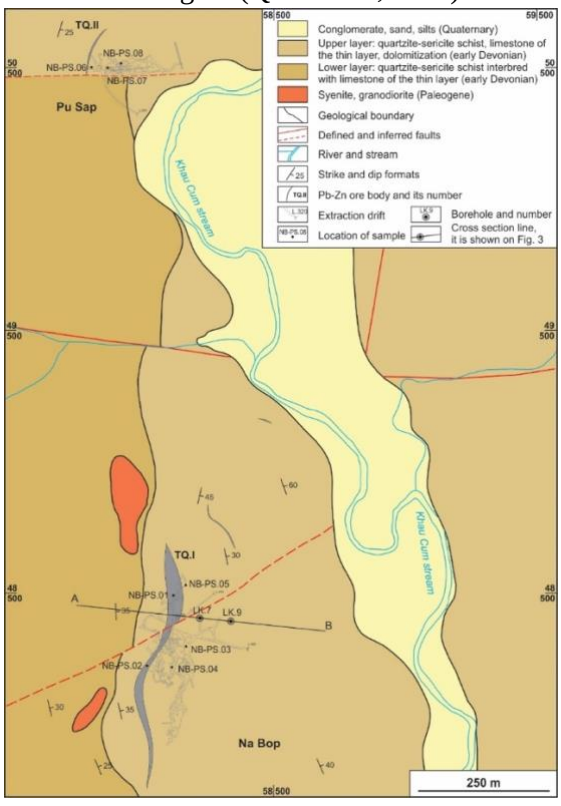

Fig. 2. Simplified geological map of the Na Bop-Pu Sap lead-zinc deposit (modified from Sang, 2010).

Intrusive magmatic rocks, including the biotite granite porphyry of the early Triassic Phia Bioc complex and the syenite rock of the Paleogene Cho Don complex, characterize the study area. These rocks are exposed as small blocks (Quoc et al., 2000). In addition, the Na Bop-Pu Sap mine site exhibits two fault systems, namely the NW-SE and NE-SW fault systems. The lead-zinc mineralization is primarily concentrated in the NW-SE fault system, with one fault acting as a conduit for ore-forming fluids. On the other hand, the NE-SW fault system intersects the TQ.1 ore body and complicates the structural characteristics of the mining area, thereby presenting challenges in the exploration and exploitation of the lead-zinc ore (Bac, 2011).

3. Samples and Analytical Methods

Eight lead-zinc ore samples were collected from the Na Bop-Pu Sap deposit and analyzed chemically and mineralogically during field survey. Among these, 5 samples (from NB-PS.01 to NB-PS.05) were used for lead isotopic analysis, and 8 samples (from NB-PS.01 to NB-PS.08) were used for sulfur isotopic analysis (Fig. 2), and more than 50 block and thin section samples were used for ore petrography analysis.

3.1. Ore Petrography

In order to analyze the mineralogy of the ore and its relationships, polished and thinly sliced rock chips were created at the Hanoi University of Mining and Geology. Utilizing a Carl Zeiss Axio Scope. A1 microscope and a scanning electron microscope (SEM) with energy-dispersive X-ray spectroscopy (EDS) technology from FEI Company, Hillsboro, OR, USA, the mineral modes were qualitatively evaluated and determined.

3.2. Sulfur Isotope Analysis

Representative ore samples were obtained, and sulfide minerals were isolated to investigate the sulfur isotope composition of sulfide minerals. The isolation process involved crushing, grinding, and sifting the samples to release unaltered pyrite and galena mineral particles, which were then hand-picked and powdered under a reflected light microscope. The resulting mineral separates were analyzed for $\delta^{34}S$ ratios at the University of Science and Technology of China using an EA1500 elemental analyzer connected to a VG/Fisons/Micromass 'Isochrom-EA' system operated in continuous He flow mode. The sample quantity tested was determined by the sulfur concentration of the sulfide material, with as little as 0.5 mg of sulfides containing 50 wt.% S (such as pyrite and marcasite) and more than 2 mg of sulfides containing 12-13 wt.% S (such as galena) being used. The samples were individually crimped in a tin capsule before being heated to 1030°C in a furnace. Flash combustion at 1800°C under a helium atmosphere with simultaneous injection of O_2 was then performed, with the resulting gases subsequently oxidized, and extra oxygen absorbed in copper wires. The gases were separated in a chromatographic column, their peaks quantified, and the SO_2 gas isolated for direct analysis in the mass spectrometer, all carried by He.

An accuracy level of 0.1 has been achieved for the $\delta^{34}S$ of sulfide minerals in this study, with reference to the Canyon Diablo Triolite (CDT). One standard is used to frequently check on the run throughout the day to guarantee the results' accuracy. Additionally, six standards spanning a range of more than 50 degrees (from -32 to +20‰) are employed to calibrate the corrections to the raw values of the samples. To further validate the calibration, one standard is analyzed for every five samples, and one blank is performed for every ten analyses to clear the system of any residual substances. It is also verified that the excess O_2 has been completely absorbed.

3.3. Lead Isotope Analysis

The MC-LA-ICP-MS Laboratory at the Institute of Geology and Geophysics, Chinese Academy of Sciences, utilized the LA-ICP-MS method to analyze the isotopic samples of Pb-Pb and U-Pb. Approximately 50 mg of rock and 50 mg of galena were employed for the U-Pb isotope ratio. The samples were then disintegrated in a mixture of HF-HClO4 in a Teflon beaker and placed in a sealed steel beaker at 180°C for six days to ensure complete digestion. The Pb was separated and purified by the conventional cation-exchange technique with diluted HBr and subsequently measured on a Finnigan MAT-262 mass spectrometer at the University of Science and Technology of China. To monitor the accuracy, the standard sample NBS SRM-981 was analyzed, yielding results of $^{206}Pb/^{204}Pb$ = 18.640-18.08, $^{207}Pb/^{204}Pb$ = 15.741-15.758 and $^{208}Pb/^{204}Pb$ = 39.160-39.336.

4. Results and Discussion

4.1 Ore and Host-Rock

The lead-zinc deposit in the study area is located within the early Devonian carbonate rocks composed of ore veins along fault zones. The primary ore veins are identified as TQ.1, TQ.2, and TQ.4 orebodies, arranged from northwest to southeast, as illustrated in Figs. 2 and 3. Bac Kan Minerals Joint Stock Company (BAMCORP) has been utilizing underground-mining methods to extract the orebodies since 2001.

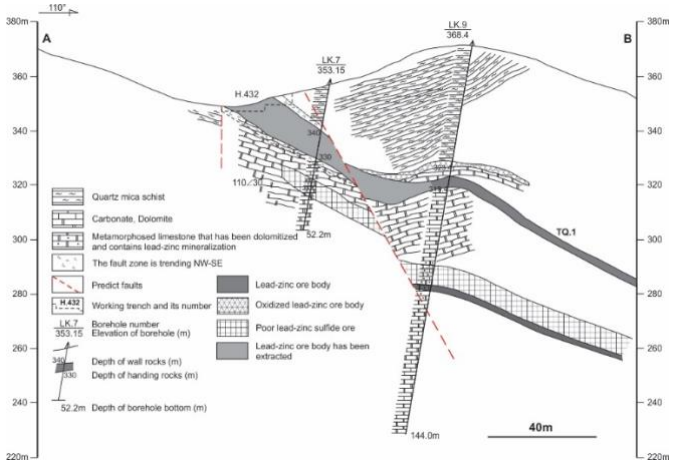

Fig. 3. Geological cross-section of the Na Bop-Pu Sap lead-zinc deposit, showing the TQ.1 lead-zinc ore body (modified from Bac, 2011).

The TQ.1 ore body, situated in the Na Bop area in the southern part of the study area, spans approximately 700m. It has an elongated north-south orientation and dips towards the east at angles ranging from 25 to 55º, which conforms to the bedding of the surrounding rock (Figs. 2, 3, and 4E, F). The surrounding rocks are primarily composed of altered limestone and dolomite. The alteration associated with the characteristic ore body includes dolomitization, chloritization, and strong dolomitization (Figs. 4C, D). The contact between the ore body and the surrounding rocks is distinct, with the thickness of the ore body varying wildly from 10.34m to 3.85m. The primary ore body is intersected by a NE-SW fault zone (Figs. 2, 3, and 4A, B), suggesting that this fault system occurred after ore mineralization and caused the displacement of the ore zones in the area. At the slip surface, limestone chips are observed, indicative of deformation, and a significant slip surface is also present in the mining area. Calcite crystals were seen to grow on the slip surfaces, although no evidence of mineralization associated with them is apparent (Figs. 4C, D).

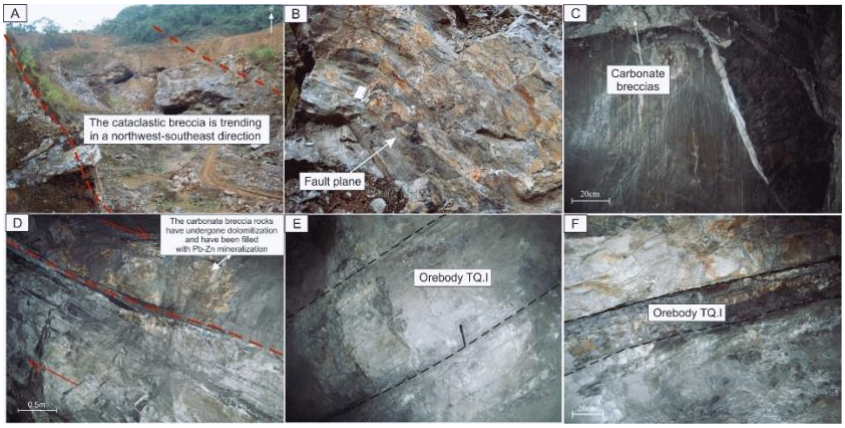

Fig. 4. Several outcrops within the Na Bop-Pu Sap deposit exhibit a fault zone and the TQ.1 lead-zinc ore body. A - The cataclastic breccia trends in an NW-SE direction at the mining area. B - A slip plane of the fault has been observed in the mining area. C - The slip plane of the fault, together with the carbonate breccia of the NE-SW fault zone, displaces the TQ.1 ore body towards the NW-SE direction. D - A quartz-calcite vein containing Pb-Zn mineralization fills the cataclastic breccia zone along the NW-SE trending fault system at level 306m of the extraction drift 320. E - The TQ.1 ore body is at level 306m of the extraction drift 320. F - The TQ.1 ore body nearly conforms to the host rock along a bedding plane.

The TQ.2 ore body is situated in the Pu Sap at the northern part of the study area, approximately 1000m away from the TQ.1 ore body in the Na Bop area. It extends 100-120m to the NE-SW direction (close to the meridian) with 35 to 40^{o} dips towards the east-northeast. The ore deposit has been fully exploited by shafts down to a depth of +219.04m. According to mining records, the thickness of the ore deposit at depth is approximately 2.5m and is relatively stable along the dip direction. The survey results indicate that the ore deposit mainly occurs in veins, filling the cracks and openings of karst caves developed along the NW-SE fault zone. On the mining surface, lead-zinc ore is observed to be extracted from karst cavities (Fig. 2). The alteration related to the ore deposit includes dolomitization and chloritization. The primary ore minerals are galena, sphalerite, pyrrhotite, pyrite, and the minor ones include arsenopyrite and chalcopyrite. The ore structure appears as disseminations, veins, and orebodies, with replacement and erosion textures. The content of Pb and Zn ores tends to decrease from top to bottom.

The TQ.4 ore body is situated in the central region of the study area, about 400m north of TQ.1, and is approximately 50-60m long in the NE-SW direction. The ore body dips steeply and intersects with altered limestone, filling fractures. The sulfide minerals pyrite, sphalerite, and galena are the primary ore minerals. Other small lead-zinc orebodies are located in both quartz-mica schists and carbonate rocks, but they have not received much attention regarding their economic viability.

4.2 Ore petrography

Microscopic investigation of thin and block sections of representative ore samples revealed that galena, pyrite, pyrrhotite, sphalerite, and arsenopyrite are the predominant ore minerals accompanied by small amounts of chalcopyrite, marcasite, hematite, argentite, tetrahedrite, tennantite, and cassiterite. Quartz, calcite, dolomite, and chalcedony occur as gangue minerals.

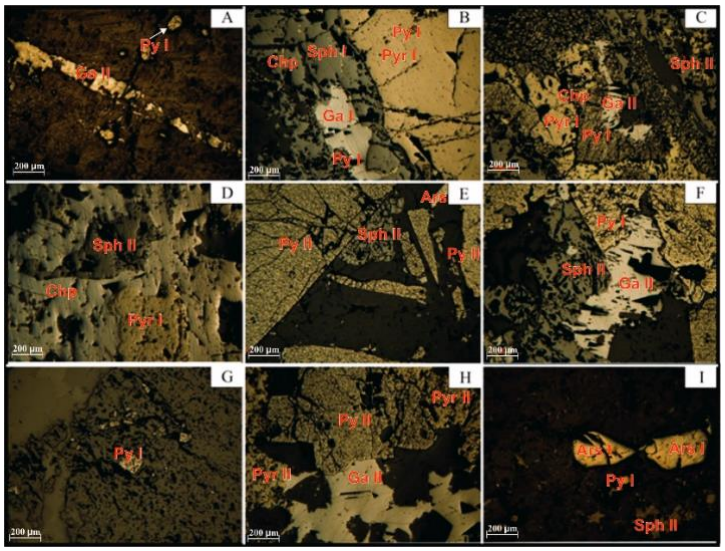

Fig. 5. Several images of the ore mineralization association in the Na Bop - Pu Sap mining area (photos taken by Ta Van Thang). A - Galena occurs as veinlets associated with pyrite, filling fractures and cavities in the rock. B - Galena I occur as small irregular grains associated with sphalerite, pyrite, and pyrrhotite, filling fractures and cavities in the rock. C - Galena II. D - Sphalerite II occurs with galena, replacing pyrrhotite. E, F - Sphalerite II. G - Pyrite is disseminated in the gangue. H - Galena is associated with pyrite. I - Arsenopyrite is broken and associated with pyrite. Py: Pyrite. Sph: Sphalerite. Ga: Galena, Chp: Chalcopyrite, Ars: Arsenopyrite, Pyr: Pyrrhotite.

Galena is an economically significant mineral in the mine, easily identifiable with the naked eye. It is usually found in association with sphalerite, chalcopyrite, and pyrite in quartz veins or quartzized/dolomitized limestone (Fig. 5D). In polished thin sections, galena is present in most samples either as thick disseminations in the limestone or as compact xenoblasts filling fractures and cavities in the rock (Fig. 5A). Galena accounts for about 20-30% of the ore minerals. Galena appears white under reflected light, with clear cleavage and triangular black inclusions visible on crystal surfaces, ranging in size from 0.1 to 1.0 mm. Galena may consist of two generations: Galena I, accounting for about 10% of total galena, occurs as small irregular grains, small platelets, or irregular grains associated with sphalerite, pyrite, pyrrhotite, and arsenopyrite, filling fractures and cavities in the rock (Fig. 5B). Galena II, constituting up to 90% of total galena, occurs as a collection of irregular grains, sometimes half-self-shaped or large platelets forming replacement veins of pyrite I, pyrrhotite I, and arsenopyrite I, with typical triangular black inclusions on their surfaces (Fig. 5C). Anglesite and cerussite, minerals formed during the supergene alteration of galena, are observed at the edges of some galena grains.

Sphalerite occurs in numerous ore samples, albeit occasionally in trace amounts; other samples represent up to 25-30% of the total ore mineral mass. It forms vein-like or interlayered structures with other sulfur minerals. Sphalerite usually exhibits black, dark brown, or gray colors, which indicate high iron content. Reflected light microscopy reveals that two generations of sphalerite are distinguishable. Sphalerite I is irregularly disseminated in the rock, occasionally filling fractures and forming veins together with galena I and pyrite I (Fig. 5B). Certain sphalerite I grain feature nucleated triangular-shaped inclusions of galena II, chalcopyrite II, and pyrrhotite II, which are the outcomes of the process of hydrothermal alteration. Sphalerite II, which is larger, is frequently found as massive aggregates, filling fractures and forming symbiotic associations with galena II and pyrite II (Figs. 5E, F).

Pyrite is a common mineral found in ores, present in most samples and occasionally in significant proportions. Pyrite particles have a distinctive shape, ranging from cubic to irregular, and vary in size from 1-3mm. Under reflected light microscopy, three types of pyrite were distinguished. Pyrite I is characterized by tabular or cubic particles, with crystal shapes ranging from cubic to irregular. Their

size ranges from 0.2mm to 2mm. Large pyrite particles may exhibit remnants of non-ore minerals. This type of pyrite is often fractured, pulverized, associated with mineral veins, and replaced by later generations of sphalerite-galena (Figs. 5F, G). Pyrite II, less common than Pyrite I, typically forms distorted or irregular particle aggregates, often fractured and jointed. It is closely associated with arsenopyrite II, pyrrhotite II, sphalerite II, and galena II (Fig. 5). Pyrite III typically consists of small cubic or irregular particles sparsely distributed in the ore vein, closely associated with calcite vein, and is less likely to be fractured or jointed.

Arsenopyrite occurs in small quantities and forms two symbiotic groups. In the first group, it is commonly found alongside pyrite and occasionally with pyrrhotite. These grains have large tabular or prismatic shapes, parallelogram shapes, etc. They are often shattered, pulverized, and fractured and are frequently filled and replaced by later generations of ore minerals, as shown in Figure 5I. In the second symbiotic group, arsenopyrite is present as small grains or aggregates with smooth surfaces and prismatic or semi-prismatic shapes. However, it is often replaced by sphalerite or galena.

Pyrrhotite is a relatively common mineral found in the Na Bop mine. There are typically two types of pyrrhotite present. Pyrrhotite I form dense clusters of prismatic or semi-prismatic grains with long tabular or parallelogram shapes closely associated with arsenopyrite and pyrite. These grains are often shattered and pulverized, and later generations of galena frequently replace their edges, as illustrated in Figures 5C, D. Pyrrhotite II is typically semi-prismatic with tabular shapes and is accompanied by small veins of quartz, calcite, and ore minerals such as galena and chalcopyrite.

Chalcopyrite occurs in insignificant quantities in some samples, either as aggregates with irregular shapes, irregularly distributed in the rock, or as pre-existing minerals.

Based on an investigation of ore mineral composition, morphology, and the relationships between these minerals in the samples, various symbiotic mineral associations have been classified at the Na Bop-Pu Sap lead-zinc deposit. The association of quartz-pyrite-arsenopyrite-pyrrhotite indicates the early hydrothermal mineralization stage, primarily resulting from the filling of cracks and exchange metamorphism between dolomitized carbonate rocks and hydrothermal fluids, as well as with the ore minerals from the preceding stage. This stage also saw the deposition of sphalerite and galena, albeit in small quantities. The association of galena-sphalerite-pyrite characterizes the industrial ore-forming stage of the orebody and often overlaps with the ore from the previous stage in space. Finally, the quartz-calcite-pyrite association represents the concluding stage of the hydrothermal mineralization process, marked by the presence of small quartz-calcite-pyrite veins cutting through the ore from the previous stage. The findings of this study aid in guiding the selection of representative sample sizes and minerals for analyzing S and Pb isotopes, as well as in accurately targeting isotopic analysis spots on the surface of ore minerals, which improves the accuracy of measurement and reduces errors.

The Pb isotopes provide information on the age of the mineralization event, while the S isotopes provide information on the source of the metals and the depositional environment (Sangster et al., 2011; Milot et al., 2019; Ünal-Çakır, 2020; Hung et al., 2021). Therefore, understanding the sulfur and lead isotopic fractionation processes that occurred during mineralization can provide insights into the geological history of the deposit, the source of the metals, and the depositional environment.

4.3 Sulfur-Isotope Studies

Sulfur-isotope analyses were carried out on galena, sphalerite, and pyrite hand-picked from ore samples, representing the various ore veins (Tab. 1).

Table 1. Sulfur-isotope compositions of galena, sphalerite, and pyrite crystals separated from the ore samples of the Na Bop-Pu Sap deposit

Sample No.	Location	$\delta^{34}S_{CDT}$‰		
		Galena	Sphalerite	Pyrite
NB-PS.01	TQ.1, Surface	4.8	6.4	5.2
NB-PS.02	TQ.1, Surface	5.3	6.8	4.6
NB-PS.03	TQ.1, 387 m sublevel	4.5	6.7	-
NB-PS.04	TQ.1, 400 m sublevel	-	-	5.8
NB-PS.05	TQ.1, 381 m sublevel	-	6.4	4.1
NB-PS.06	TQ.2, 324 m sublevel	1.3	-	-
NB-PS.07	TQ.2, 302 m sublevel	0.1	2.5	-
NB-PS.08	TQ.2, 296 m sublevel	0.7	3.2	-

The $\delta^{34}S_{CDT}$ values of galena, sphalerite, and pyrite exhibit a range of 0.1‰ to 5.3‰ (average 2.8‰), 2.5‰ to 6.8‰ (average 5.3‰), and 4.1‰ to 5.8‰ (average 4.9‰), respectively. The $\delta^{34}S$ values are positive, and the variation in $\delta^{34}S$ values within a certain range is significant, indicating that the sulfur isotopic composition is unstable. Specifically, the $\delta^{34}S$ values of pyrite were found to be less than those of sphalerite (ranging from 2.5‰ to 6.8‰), with a range of 4.1‰ to 5.8‰. This phenomenon may be attributed to the fact that the sulfur fraction did not reach equilibrium during the evolution of the hydrothermal system, or it may be due to the loss of $\delta^{34}S$ in the ore-forming fluid caused by the high oxygen fugacity in the evolution of the hydrothermal fluid (Pirajno, 2009).

Fig. 6 depicts a schematic of the $\delta^{34}S$ isotope values, providing information about the sources of the ore-forming materials. Based on this diagram, it can be concluded that most lead-zinc ore formations originated from marine sedimentary deposits and granite. Figure 7 illustrates the key ore-forming origins, revealing that massive sulfide deposits housed by sediments, such as the Red-bed and MVT types, were the primary source of lead-zinc ore formations.

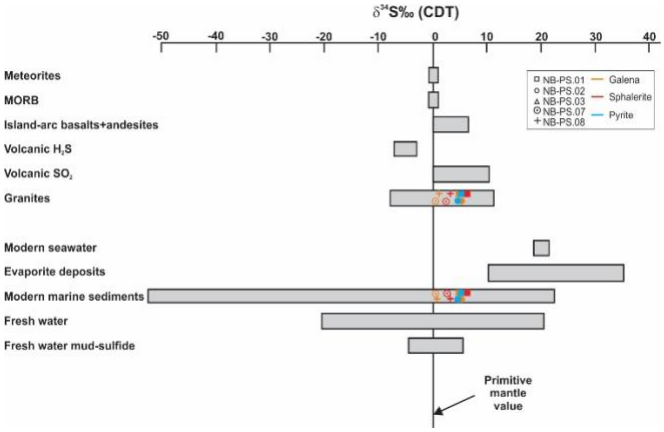

Fig. 6. Natural sulfur isotope reservoirs, showing lead-zinc forming material sources in the Na Bop-Pu Sap deposit (data from Coleman 1977, Claypool et al. 1980, Chambers 1982, Sakai et al. 1982, Kerridge et al. 1983, Ueda & Sakai 1984, Chausidon et al. 1989).

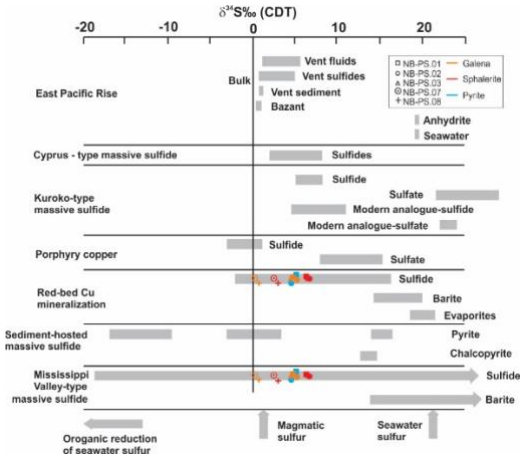

Fig. 7. The $\delta^{34}S$ values for sulfur-bearing minerals in hydrothermal deposits, showing the lead-zinc deposits of the Na Bop-Pu Sap deposit (data from Ohmoto & Rye 1979, Eldridge et al. 1988, Kerridge et al. 1988, and Naylor et al. 1989).

However, the observed $\delta^{34}S$ values in Table 1 display a narrow range of variation, indicating that the minerals originated from a singular ore-forming source. The $\delta^{34}S$ values of the sulfide ore assemblage were consistently <10‰, with three galena values <1.5‰ and approaching 0‰. This suggests that the sulfide mineralization might be linked to a deep-seated source, likely associated with magmatic activity in the region (Fig. 6), and possibly influenced by carbonate-bearing marine sedimentary rocks (Fig. 7; Pirajno, 2009; Duan et al., 2016; Gill et al., 2019).

4.4 .Lead-Isotope Studies

Lead-isotope analyses were performed on galena, sphalerite, and pyrite separated from the ore samples. Table 2 provides the lead-isotope data for eight ore samples from various levels of the ore veins (TQ.1 and TQ.2) dispersed over narrow ranges, from 18.749 to 18.783 for $^{206}Pb/^{204}Pb$, from 15.677 to 15.713 for $^{207}Pb/^{204}Pb$, and from 38.895 to 38.992 for $^{208}Pb/^{204}Pb$.

Table 2. Lead-isotope compositions of galena, sphalerite, and pyrite from the Na Bop-Pu Sap deposit.

Sample No.	Minerals	$^{208}Pb/^{204}Pb$ (*)	$^{207}Pb/^{204}Pb$ (*)	$^{206}Pb/^{204}Pb$ (*)	Model age (Ma)
NB-PS.01	Galena	39.142	15.730	18.564	510
NB-PS.01	Pyrite	39.425	15.815	18.632	424
NB-PS.01	Sphalerite	39.329	15.787	18.612	586
NB-PS.02	Galena	39.196	15.746	18.578	531
NB-PS.02	Pyrite	39.501	15.836	18.651	448
NB-PS.02	Sphalerite	39.235	15.758	18.588	547
NB-PS.03	Galena	39.356	15.794	18.615	598
NB-PS.03	Sphalerite	39.323	15.787	18.606	590
NB-PS.04	Pyrite	38.909	15.685	18.451	503
NB-PS.05	Sphalerite	39.333	15.789	18.605	595

Note: (*) an external reproducibility for lead-isotopic ratios is 0.1% for $^{206}Pb/^{204}Pb$, 0.15% for $^{207}Pb/^{204}Pb$, and 0.2% for $^{208}Pb/^{204}Pb$ at the 2σ confidence level.

The plumbotectonics model, as proposed by Zartman and Doe (1981), can be utilized to determine the source of Pb. The $^{208}Pb/^{204}Pb$ vs. $^{206}Pb/^{204}Pb$ and $^{207}Pb/^{204}Pb$ vs. $^{206}Pb/^{204}Pb$ diagrams (Fig. 8) indicate that the Pb isotopic composition data were projected on the lower crust.

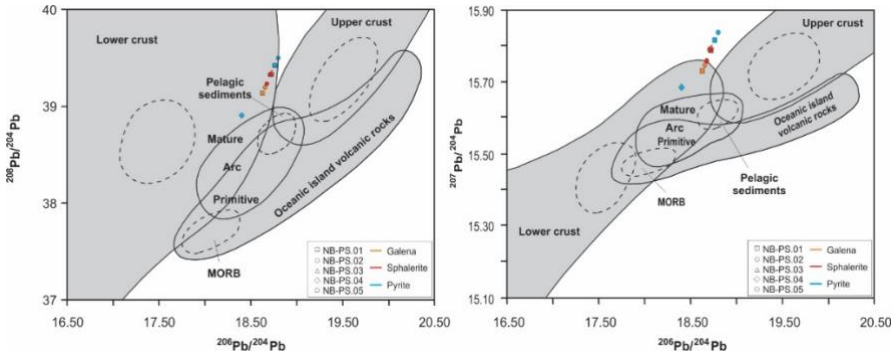

Fig. 8. Plot of Pb isotope data from the Na Bop-Pu Sap area on $^{208}Pb/^{204}Pb$ vs $^{206}Pb/^{204}Pb$, and $^{207}Pb/^{204}Pb$ vs $^{206}Pb/^{204}Pb$ diagrams. The dotted line indicates each area of greatest concentration (after Zartman & Doe 1981). Oceanic Island Volcanic Rocks and MORB represent the Mantle area, and Arc and Pelagic Sediments represent the Orogen area.

Utilizing the Pb isotope model developed by Stacey and Kramers (1975), the calculated model ages range from 424 to 598 Ma with a median of 539 Ma, signifying a Neoproterozoic to Cambrian age (Table 2). This age range is similar to the one recently suggested for the occurrence of lead-zinc mineralization in the Cho Don-Cho Dien area (Hung et al., 2021) and is concurrent with the Jinning episode, which could have resulted from the Late Proterozoic collision between the Cathaysia and Yangtze plates (Golonka et al., 2006). Other events may have been triggered by the early effects of the mantle plume that initiated the disintegration of Rodinia (Li et al., 1999), or the earliest collisions that led to the creation of Gondwana (Metcalfe, 2006), culminating in a unified Palaeo-South China plate. As a result, the radiogenic Pb probably got stored in Proterozoic rocks before being mobilized and redeposited in Devonian rocks within the investigated area. The claim that Pb-Zn ores are genetically linked to early Triassic granitoid of the Phia Bioc complex is improbable, given the significant challenge of Pb extraction from its source approximately 500 Ma ago and subsequent differentiation over almost 300 Ma, resulting in ore deposit formation. The statement suggests that the faults and mineralization that contain ores within the studied region existed before granitoid emplacement during the early Triassic period.

4.5. Genesis Model

The research results indicate that the lead-zinc ore in the Na Bop-Pu Sap deposit exhibits characteristics of carbonate-hosted hydrothermal ore deposits. The lead-zinc mineralization is controlled by fault zones that exhibit ductile deformation along the fractures in the region. Sulfur and lead isotopic analyses have revealed that the source material for the sulfur that formed the lead-zinc mineralization is derived from a deep-seated source related to magmatic activity during the Neoproterozoic to Cambrian period in the Cho Don area, which mixed with the carbonate sedimentary rocks in the crust. The fault systems in the crust act as channels for the destruction of Devonian carbonate rocks. These rocks are dissolved by ascending magmatic fluids, mixed with surrounding rocks, and deposited in favorable structural traps.

The ICP-MS analysis results of the samples retrieved from the TQ.1 ore body reveal that the lead concentration surpasses that of zinc. Conversely, the concentration of Pb is lower than that of Zn in the TQ.2 ore body, as reported by Sang (2010). Moreover, the research data on the isotopes of sulfur and lead suggest that the origin of the ore-forming materials is more closely linked to the magma activity occurring at greater depths rather than the separation from the sources of carbonate rocks surrounding the ore body or the process of exhalation under the seafloor.

The Na Bop-Pu Sap deposit is notable for the presence of ores not only in the primary ore-hosting strata but also in ore-bearing faults, which indicates a connection between the ore-hosting strata, ore-bearing faults, and orebodies. The geological features of the deposit share many similarities with MVT deposits, including tectonic setting, host rock type, wall rock alteration style, and mineral composition (Hoa et al., 2010; Niem, 2010). However, the Na Bop-Pu Sap Pb-Zn deposit also displays several distinct geological characteristics that differ from those of typical MVT deposits, such as the unique ore-controlling structure, lithological character, relationship to magmatic rocks, ore texture, and structure, model age of lead-zinc mineralization and host rocks, among others (Binh et al., 2010; Can et al., 2014). Based on the structures and textures of the lead-zinc ore observed in the field and studied in the laboratory, as well as in subsequent research, these suggest that the Na Bop-Pu Sap lead-zinc deposits do not exhibit characteristics of either MVT or SEDEX types. However, they appear to be related to shear zone-hosted lead-zinc deposits.

5. Conclusions

- The study investigates the genesis of lead-zinc deposits and the sources of ore-forming material in the Na Bop-Pu Sap Pb-Zn deposits, Cho Don area, northeastern Vietnam, using sulfur and lead isotopes. The study draws the following conclusions.
- Microscopic analyses of the veins reveal the presence of galena, sphalerite, chalcopyrite, pyrite, arsenopyrite, and pyrrhotite as ore minerals, and quartz, calcite, dolomite, and chalcedony as gangue minerals.
- The results of the sulfur isotope analysis suggest that the sulfide mineralization may be related to a deep source, possibly originating from magmatic activity in the region and contaminated by carbonate-bearing marine sedimentary rocks.
- Lead-isotope studies indicate a model age of 598-424 Ma for the lead reservoir, which is consistent with the possible presence of local source rocks containing sulfur. The lead and sulfur in the ore veins were likely contaminated by Devonian carbonate-bearing marine sedimentary rocks and leached from Neoproterozoic to Cambrian magmatic activity. Furthermore, the Na Bop-Pu Sap lead-zinc deposits do not exhibit characteristics of either MVT or SEDEX types and appear to be related to shear zone-hosted lead-zinc deposits. These findings suggest that the evolution of ore-forming materials for lead-zinc mineralization occurs at a deeper source, which is crucial in understanding the mineralization potential of these deposits.

Acknowledgements

Authors gratefully acknowledge the support of the Vietnam Ministry of Education and Training (VMOET) under grant number B2023-MDA-08. Our thankful express our appreciation to the Editors and Reviewers for their valuable feedback.

References

Anh, T.T., Gaskov, I.V., Hoa, T.T., Nevol'ko, P.A., Dung, P.T., Can, P.N., 2012. Complex Deposits in the Lo Gam Structure, Northeastern Vietnam: Mineralogy, Geochemistry, and Formation Conditions. Russian Geology and Geophysics, 53(7): 623-35.

Bac, D.T., 2011. Research on characteristics and distribution regularities of lead-zinc metallogenic formations in the Viet Bac area, Northern Vietnam. Ph.D. Thesis, Hanoi University of Mining and Geology, Ph.D. Thesis, Hanoi (in Vietnamese).

Binh, D.Q., Cuong, D.Q., Chinh, K.T., Hung, N.M. & Que, N.T., 2005. Report on prospective results of lead-zinc, gold, and accompanying minerals of the Phia Da-Na Cang area, Cao Bang-Bac Kan provinces. Vietnam Institute of Geosciences and Mineral Resources, Ha Noi, 193 (in Vietnamese).

Binh, D.Q., Cuong, D.Q., Dong, N.C., De, P.Q., Linh, N.T.H., Que, N.T. & San, V.T., 2010. Report on prospective results of copper, lead-zinc, and accompanying minerals of the Quang Ba-Pac Nam area, Ha Giang province. Vietnam Institute of Geosciences and Mineral Resources, Ha Noi, 179 (in Vietnamese).

Can, P.N., Ishiyama, D., Anh, T.T., 2014. Mineralization of indium in northern Vietnam: A study on mineralogy and geochemistry of the Na Bop and Lung Hoai Deposits in the Cho Don and Cho Dien Mining Area. Acta Geologica Sinica 88(s2): 194-196.

Chambers, L.A., 1982. Sulfur isotope study of a modem intertidal environment and the interpretation of ancient sulfides. Geochimica et Cosmochimica Acta, 46, 721-728.

Chaussidon, M., Albarede, F. & Sheppard, S.M.F., 1989. Sulfur isotope variations in the mantle from ion microprobe analyses of micro-sulphide inclusions. Earth and Planetary Science Letters, 144-156. https://doi.org/10.1016/0012-821X%2889%2990042-3.

Claypool, G.E., Helser, W.T., Kaplan, I.R., Sakai, H. & Zak, I., 1980. The age curves of sulfur and oxygen isotopes in marine sulfate and their mutual interpretation. Chemical Geology, 28, 199-260. https://doi.org/10.1016/0009-2541(80)90047-9.

Coleman, M.L., 1977. Sulphur isotopes in petrology. Journal of the Geological Society, 133, 593-608. https://doi.org/10.1144/gsjgs.133.6.0593.

Duan, J., Tang, J., Lin, B., 2016. Zinc and lead isotope signatures of the Zhaxikang Pb-Zn deposit, South Tibet: Implications for the source of the ore-forming metals. Ore Geology Reviews, 78, 58-68. http://dx.doi.org/10.1016%2Fj.oregeorev.2016.03.019.

Duong, V.H., Phan, T.T., Nguyen, T.D., Piestrzyski, A., Nguyen, D.C., Pieczonka, J., Ngo, X.D., Phong, T.V., Pham, T.B., Huong, N.V., Ngo, V.L., Bui, T.D., Vu, D.K., Bui, C.T., 2021. Cu-Au mineralization of the Sin Quyen deposit in north Vietnam: A product of Cenozoic left-lateral movement along the Red River shear zone. Ore Geology Reviews, 132, 1-21, 104065.

Eldridge, C.S., Compston, W., Williams, I.S., Both, R.A., Walshe, J.L. & Ohmoto, H., 1988. Sulfur isotope variability in sediment-hosted massive sulfide deposits as determined using the ion-microprobe, SHRIMP: I. An example from the Rammelsberg orebody. Economic Geology, 83, 443-449. https://doi.org/10.2113/gsecongeo.83.2.443.

Gill, S., Piercey, S., Layne, G.D. & Piercey, G.D., 2019. Sulphur and lead isotope geochemistry of sulphide minerals from the Zn-Pb-Cu-Ag-Au Lemarchant volcanogenic massive sulphide (VMS) deposit, Newfoundland, Canada. Ore Geology Reviews, 104, 422-435. http://dx.doi.org/10.1016/j.oregeorev.2018.11.008.

Golonka, J., Krobicki, M., Pająk, J, Giang, N.V. & Zuchiewicz, W., 2006. Global plate tectonics and paleogeography of Southeast Asia. Faculty of Geology, Geophysics and Environmental Protection, AGH-University of Science and Technology; Arkadia, Kraków, 128 pp.

Hoa, T.T., Anh, T.T., Dung, P.T., Hung, T.Q., Nien, B.A, Hieu, T.V., & Can, P.N., 2010. By-products in lead-zinc and copper ores of Northeast Vietnam. Journal of Earth Sciences, 32(4), 289-298 (in Vietnamese).

Hoa, T.T., Izokh, A.E., Polyakov, G.V., Borisenko, A.S., Anh, T.T., Balykin, P.A., Phuong, N.T., Rudnev, S.N., Van, V.V. & Nien, B.A., 2008. Permo-Triassic magmatism and metallogeny of Northern Vietnam in relation to the Emeishan plume. Russian Geology and Geophysics, 49, 480-491.

Hung, K.T., 2021. An overview of some dating methods of mineralization. Journal of Mining and Earth Sciences, 62 (2), 25-34 (in Vietnamese, English abstract).

Hung, K.T., Sang, P.N., Phuong, N., Dung, N.T., Bac, B.H., Phi, N.Q., Sang, B.V., 2020a. Polymetallic nodules resource estimation in the Suoi Thau-Sang Than Area, northeastern Vietnam. Inżynieria Mineralna, Journal of the Polish Mineral Engineering Society, 1 (2), 1-14.

Hung, K.T., Sang, P.N., Phuong, N., Linh, V.T. & Sang, B.V., 2020b. Statistical evaluation of the geochemical data for prospecting polymetallic mineralization in the Suoi Thau-Sang Than region, Northeast Vietnam. Geology, Geophysics and Environment, 46, 285-299.

Hung, K.T., Tung, T.D., Binh, D.Q., Sang, P.N., Cuc, N.T., Linh, N.T.H., Tin, Q.D., 2021. Sulfur and lead isotope geochemical characteristics of Pb-Zn deposits in the Khau Loc zone, northeastern Vietnam, and their significance. Journal of Geology, Geophysics & Environment 47(3), 143-157.

Ishihara, S., Tuan-Anh, T., Yasushi, W., & Trong-Hoa, T., 2010. Chemical characteristics of lead-zinc ores from North Vietnam, with a special attention to the in contents. Bulletin of the Geological Survey of Japan, 61, 307-23.

Kerridge, J.F., Chang, S. & Shipp, R., 1988. Deuterium exchange during acid-demineralization. Geochimica et Cosmochimica Acta, 52, 2251-2255.

Kerridge, J.F., Haymon, R.M. & Kastner, M., 1983. Sulfur isotope systematics at the 21oN site, East Pacific Rise. Earth and Planetary Science Letters, 66, 91-100.

Leach, D.L., 2005. Sediment-hosted lead-zinc deposits: A global perspective. Economic Geology, 100, 561–607.

Li, Z.X., Li, X.H., Kinny, P.D. & Wang, J., 1999. The breakup of Rodinia: Did it start with a mantle plume beneath South China? Earth and Planetary Science Letters, 173, 171-181.

Metcalfe, I., 2006. Palaeozoic and Mesozoic tectonic evolution and palaeogeography of East Asian crustal fragments: The Korean Peninsula in context. Gondwana Research, 9, 24-46.

Milot, J., Blichert-Toft, J., Sanz, M.A., Fetter, N., Télouk, P., & Albarède, F., 2021. The significance of galena Pb model ages and the formation of large Pb-Zn sedimentary deposits. Chemical Geology, 583, 120-444.

Naylor, H., Turrier, P., Vaughan, D.J., Boyce, A.J. & Fallick, A.E., 1989. Genetic studies of redbed mineralization in the Triassic of the Cheshire basin, northwest England. Journal of the Geological Society, 146, 685-699.

Niem, N.V., 2010. Establishing a scientific basis for constructing models of lead-zinc ore genesis in Northern Vietnam. Project of the Ministry of Natural Resources and Environment (in Vietnamese).

Ohmoto, H. & Rye, R.O., 1979. Isotopes of sulfur and carbon. [Inin:] Barnes, H.L. (ed.), Geochemistry of hydrothermal ore deposits. Wiley, New York, 509-567.

Pirajno, F., 2009. Hydrothermal Processes and Mineral Systems. Springer, 1249.

Quoc, N.K. (ed.), 2000. Report on results of geological mapping and mineral investigation of Bac Kan sheet at 1:200.000 scale. Geological Department of Vietnam, Hanoi (in Vietnamese).

Sakai, H., Casadevall T.J., & Moore J.G., 1982. Chemistry and isotope ratios of sulfur in basalts and volcanic gases at Kilauea volcano, Hawaii. Geochimica et Cosmochimica Acta, 46, 729-738.

Sang, B.V. (ed.), 2010. Report on lead-zinc ore exploration in the Na Bop-Pu Sap area, Chon Don district, Bac Kan province. General Department of Geology and Minerals of Vietnam, Hanoi (in Vietnamese).

Sangster, D., Outridge, P.M., & Davis, W., 2011. Stable lead isotope characteristics of lead ore deposits of environmental significance. Environmental Reviews, 8, 115-147.

Stacey, J.S., Kramers, J.D., 1975. Approximation of terrestrial lead isotope evolution by a two-stage model. Earth and Planetary Science Letters 26, 207-221.

Tri, T.V. & Khuc, V. (ed.), 2011. Geology and Earth Resources of Vietnam. General Department of Geology and Minerals of Vietnam, Publishing House for Science and Technology, Hanoi.

Ueda, A., & Sakai, H., 1984. Sulfur isotope study of Quaternary volcanic rocks from the Japanese islands arc. Geochimica et Cosmochimica Acta, 48, 1837-1848.

Ünal-Çakır, E., 2020. Sulphur and lead isotope geochemistry of the Dursunbey (Balıkesir) lead-zinc deposit. Journal of African Earth Sciences, 172, 104003.

Vinh, N.K., 1982. Radioactive age and metallogenic specialization of Phia Bioc granite complex based on geochemical and lead isotope data. Geological Journal, 154, 23-25 (in Vietnamese).

Vladimirov, A.G., Balykin, P.A., Anh, P.L., Kruk, N.N., Phuong, N.T., Travin, A.V., Hoa, T.T., Annikova, I.Yu., Kuybida, M.L., Borodina, E.V., Karmysheva, I.V., Nien, B.A., 2012. The Khao Que - Tam Dao gabbro - granite massif, Northern Vietnam: A petrological indicator of the Emeishan Plume. Russian Journal of Pacific Geology, 6 (5), 395-411.

Wilkinson, J.J., 2013. Sediment-hosted zinc-lead mineralization: Processes and perspectives. Treatise on Geochemistry, 13, 219-249.

Zartman, R.E., & Doe, B.R., 1981. Plumbotectonics - The model. Tectonophysics 75, 135-162.